Journal of NeuroVirology (1998) 4, 606–618

http://www.jneurovirol.com

Regional changes in 5-HT_{1A} but not in 5-HT_{2A} receptors in mouse brain after Semliki Forest virus infection: radioligand binding and autoradiographic studies

Surekha Mehta and Ian Kitchen

Pharmacology Research Group, School of Biological Sciences, University of Surrey, Guildford, Surrey GU2 5XH, UK

Dysfunction of brain 5-hydroxytryptaminergic systems has been associated with several neurological and psychiatric diseases which may have a viral aetiology. The effect of Semliki Forest virus (SFV) on 5-hydroxytryptamine (5-HT_{1A} and 5-HT_{2A}) receptors in mouse brain has been assessed by membrane homogenate binding and autoradiography. Adult mice were injected with saline or virus and brains removed 2, 6, 14, 22 and 35 days after infection. 5-HT_{1A} and 5-HT_{2A} receptors were characterised by saturation studies using [^{3}H] 8-OH-DPAT and [^{3}H] Ketanserin respectively. SFV infection increased 5-HT_{1A} receptor numbers by up to 80% in the cortex on days 6, 14, and 22 but had no effect on B_{max} in the midbrain, pons/medulla and the hypothalamus. SFV infection did not affect 5-HT_{2A} receptor number in any of the brain regions studied and the affinity (K_d) of either ligand for 5-HT_{1A} or 5-HT_{2A} receptors was unaffected. Autoradiographic mapping of 5-HT_{1A} receptors in SFV-infected brain showed substantially higher binding in nucleus accumbens, tenia tecta, septohippocampal nucleus, septum, medial and basolateral amygdaloid nucleus, anterioventral preoptic nucleus, hippocampus, interpeduncular nucleus, frontal, lateral orbital, and entorhinal cortex and claustrum on days 6 and 14. Elevated binding persisted in tenia tecta, frontal, lateral orbital, entorhinal cortex, and hippocampal formation to day 22. Autoradiography of 5-HT_{2A} receptors using [^{3}H] Ketanserin showed no difference in the binding in SFV-infected brains. A decrease in plasma corticosterone levels in SFV-infected mice was observed on post infection days 6 and 22. These results show SFV infection induces a regionally selective upregulation of 5-HT_{1A} but not 5-HT_{2A} receptors.

Keywords: Semliki Forest Virus; 5-HT_{1A} receptors; 5-HT_{2A} receptors; corticosterone

Introduction

The 5-hydroxytryptamine system in the brain has been associated with a variety of neurological and psychiatric diseases including anxiety, depression, schizophrenia (Grahame-Smith, 1992) and Chronic Fatigue Syndrome (CFS) (Bakheit *et al*, 1992). In addition, it has been suggested that CFS is preceded by viral infection and the resulting clinical symptoms such as muscle fatigue, impairment of cognitive function, sleep disturbance and weight loss may be due to a dysfunction in the 5-hydroxytryptamine (5-HT) system (Bakheit *et al*, 1992; Gow *et al*, 1991; Natelson *et al*, 1994). Recently, there have been reports that several viruses are capable of interfering with neurotransmitters. Behavioural deficits due to 5-HT depletion in adult rat brain after vesicular stomatitis virus infection have been reported (Mohammed *et al*, 1990) and rabies virus has been shown to induce downregulation of 5-HT_{1D} like receptors without an effect on 5-HT_{1A}, $_{1B}$ or $_{2C}$ receptors (Ceccaldi *et al*, 1993). During an acute experimental brain infection by herpes simplex virus type 1 in rabbits, increased homovanillic acid concentration and decreased dopamine D_2 receptor number have been shown (Paivarinta *et al*, 1992). We now report, in a mouse model, the effects of Semliki Forest Virus (SFV)

Correspondence: I Kitchen
Received 15 January 1998; revised 8 June 1998; accepted 26 June 1998

infection on 5-HT$_{1A}$ and 5-HT$_{2A}$ receptor subtypes as they have been clearly implicated in mood and behaviour and also in sleep and appetite functions (Baxter *et al*, 1995; Whitaker-Azmitia and Peroutka, 1990) to determine if these receptor proteins are targets for some viruses and thus may be responsible for behavioural symptomatology in some CNS diseases. The avirulent strain of SFV is neuroinvasive in adult mice after a single intraperitoneal inoculation without producing a clinical illness such as paralysis, hunch back and fur ruffling. The histopathological changes include microcystic changes, perivascular cuffing and demyelination which is immune mediated and T-cell dependent (Illavia *et al*, 1982, 1998; Fazakerley *et al*, 1983; Pathak *et al*, 1983).

Results

The effect of SFV on 5-HT$_{1A}$ and 5-HT$_{2A}$ receptors in mouse brain was assessed 2, 6, 14, 22 and 35 days

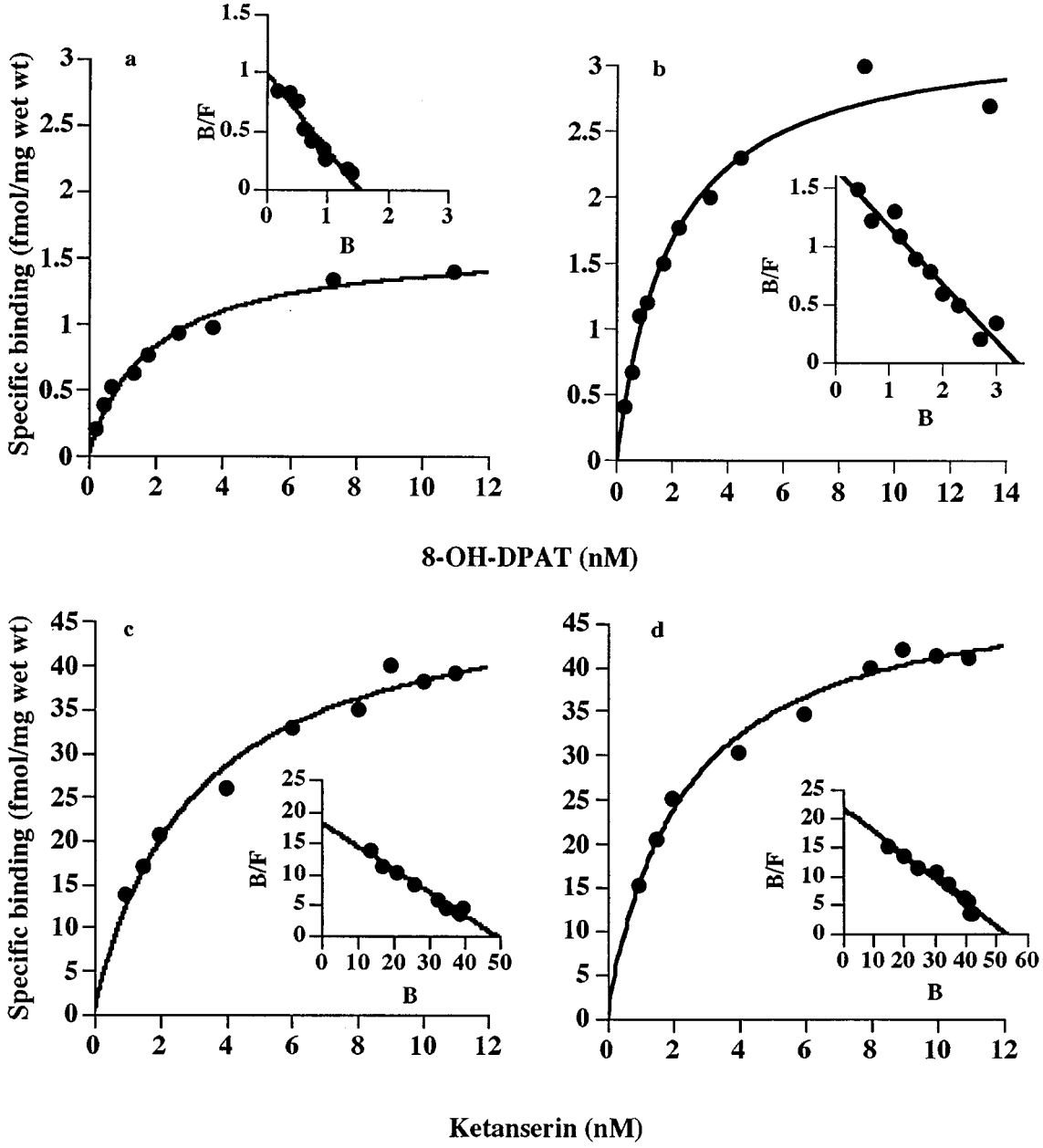

Figure 1 Saturation binding characteristics of [^{3}H] 8-OH-DPAT (upper graphs) and [^{3}H] Ketanserin (lower graphs) in cortex on day 6 after saline-treatment (a and c) and SFV infection (b and d). The inset shows a Scatchard plot derived from the specific binding data. B=Bound, F=Free.

after infection. Homogenate binding studies were used to determine the effect of SFV on receptor affinity and maximal number of binding sites in four brain regions. In addition, to determine the anatomical sites of action of SFV upon 5-HT receptors, quantitative autoradiography was also performed on brain sections taken from SFV infected mice at day 6, 14 and 22.

Effect of SFV infection on 5-HT$_{1A}$ receptors: Homogenate binding

[^{3}H] 8-OH-DPAT displayed high-affinity saturable single site binding in all the four regions of the brain studied. The mean binding curves and Scatchard transformations after saline-treatment and SFV infection on day 6 in cortex are shown in Figure 1a and b. The maximum binding capacity (B_{max})

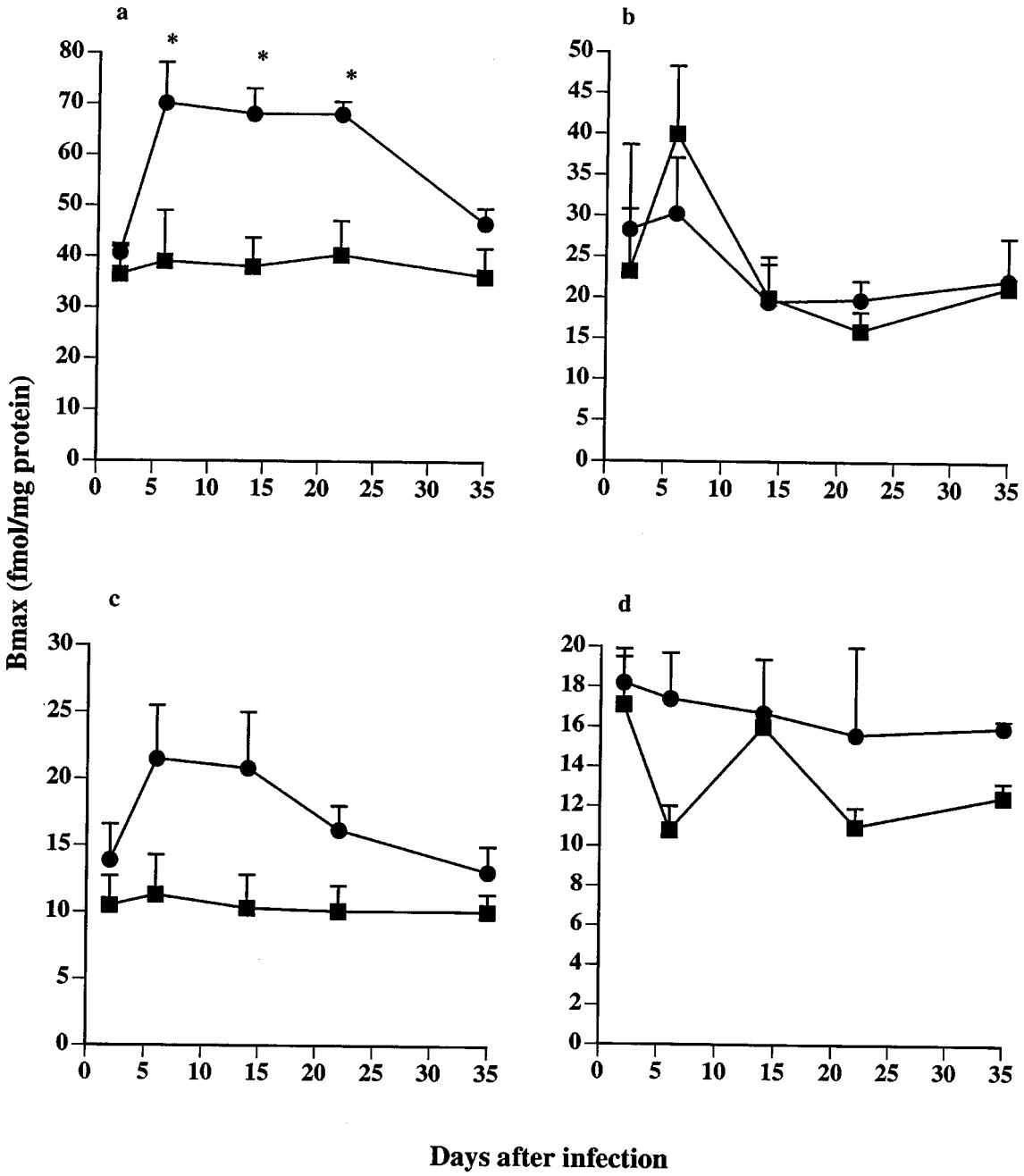

Figure 2 Time course of the effect of SFV on the number of 5-HT$_{1A}$ receptors labelled with [^{3}H] 8-OH-DPAT. Values represent Bmax (fmol/mg protein). (**a**) cortex, (**b**) mid brain, (**c**) hypothalamus, and (**d**) pons/medulla on various days after infection. ● SFV, ■ Saline. *denotes significant difference ($P<0.05$) from values in saline-treated mice. Comparisons were made by 2-way ANOVA. Specific comparisons of SFV and saline treatment were made at each age using Duncan's *post hoc* test. n=4. Error bars show s.e.m.

during SFV infection was increased by 80% in the cortex compared to the saline-treated group (Figure 2a) 6 days after infection, remaining elevated on days 14 and 22 and returning to the control value by day 35 (Figure 2a). In the SFV-infected group, an increased binding of [^{3}H] 8-OH-DPAT was measured in the hypothalamus but did not reach significance (Figure 2c). There was no difference in B_{max} between SFV-infected and saline-treated groups in the midbrain and pons/medulla at any time points (Figure 2b and d). The affinity constant (K_d) for [^{3}H] 8-OH-DPAT during SFV infection in cortex, midbrain, pons/medulla and hypothalamus was comparable to the K_d derived in the parallel regions of saline-treated brains on each post infection day (Table 1). For all determinations the effects of SFV were equivalent when expressed per wet weight tissue or per protein and SFV had no significant effect on brain protein levels (data not shown).

Effect of SFV infection on 5-HT$_{1A}$ receptors: Autoradiography

The regional distribution of [^{3}H] 8-OH-DPAT in mouse brain in saline-treated and SFV infected animals is shown in Figure 3. Table 2 shows the quantitative regional binding of [^{3}H] 8-OH-DPAT in the mouse brain on various days after infection. 5-HT$_{1A}$ binding sites were heterogeneously distributed in both saline-treated and SFV-infected brains, being particularly abundant in the claustrum, septum, hippocampus (CA2 > CA1), entorhinal cortex and interpeduncular nucleus. Intermediate levels were detected in most cortical regions (frontal, orbital, parietal, cingulate, piriform, oculomotor, temporal), anterior olfactory nucleus and taenia tecta, septohippocampal nucleus, dentate gyrus and dorsal raphe nucleus. Lower levels were detected in retrosplenial cortex, central gray, hypothalamus, nucleus accumbens, amygdaloid nucleus and media raphe nucleus. A higher density of binding in SFV-infected groups was measured in nucleus accumbens, tenia tecta, septohippocampal nucleus, septum, medial and basolateral amygdaloid nucleus, anteroventral preoptic nucleus, hippocampus including CA1, CA2, interpeduncular nucleus, frontal, lateral orbital, and entorhinal cortex and claustrum on days 6 and 14. In several of these regions SFV infection caused a doubling of the number of receptors labelled. On day 22, binding in some regions (tenia tecta, frontal, lateral orbital, entorhinal cortex, and hippocampus) was still elevated in SFV-infected brains (Table 2).

Effect of SFV infection on 5-HT$_{2A}$ receptors: Homogenate binding

[^{3}H] Ketanserin displayed high-affinity saturable single site binding in all the four regions of the brain studied. The mean binding curves and Scatchard transformations after saline-treatment and SFV infection on day 6 in cortex are shown in Figure 1c and d. There was no significant difference in the number (B_{max}) or affinity (K_d) of 5-HT$_{2A}$ receptors labelled with [^{3}H] Ketanserin between SFV-infected and saline-treated mice in any brain regions up to 35 days after infection (Figure 4a–d, Table 1). For all determinations the effect of SFV were equivalent when expressed per wet weight tissue or per protein and SFV had no significant effect on brain protein levels (data not shown).

Effect of SFV infection on 5-HT$_{2A}$ receptors: Autoradiography

The regional distribution of 5-HT$_{2A}$ receptors labelled with 4 nM [^{3}H] Ketanserin in mouse brain is shown in Figure 5 and a quantitative analysis is shown in Table 3. There was no significant

Table 1 Effect of SFV on the affinity (K_d, nM) of [^{3}H] 8-OH-DPAT for 5-HT$_{1A}$ and [^{3}H] Ketanserin for 5-HT$_{2A}$ receptors in adult mouse brain.

	Cortex		*Mid brain*		*Pons/medulla*		*Hypothalamus*	
PID	*SFV*	*Saline*	*SFV*	*Saline*	*SFV*	*Saline*	*SFV*	*Saline*
5-HT$_{1A}$								
2	1.3±0.08	1.5±0.11	1.6±0.09	2.2±0.49	2.6±0.33	2.6±0.26	3.1±0.49	2.7±0.63
6	1.3±0.45	1.8±0.17	2.1±0.37	2.2±0.50	2.6±0.41	2.4±0.22	2.7±1.08	2.1±0.60
14	1.5±0.12	1.8±0.02	1.5±0.11	2.2±0.05	2.9±0.11	2.1±0.22	3.2±0.23	2.9±0.23
22	1.4±0.12	1.6±0.09	1.7±0.19	2.4±0.48	2.9±0.36	2.4±0.47	2.6±0.33	2.9±0.40
35	2.0±0.10	2.3±0.30	1.8±0.30	2.0±0.20	2.8±0.50	2.0±0.09	3.3±0.24	2.8±0.35
5-HT$_{2A}$								
2	2.4±1.50	2.8±0.49	2.0±2.20	2.4±3.20	2.1±1.20	1.9±2.40	3.6±0.70	2.6±0.50
6	2.9±1.30	1.4±0.22	1.5±1.50	2.2±3.40	5.5±4.30	4.2±0.45	4.2±0.70	2.8±0.60
14	3.1±0.23	2.5±0.60	3.4±4.60	2.0±2.50	2.0±3.40	1.4±2.20	5.8±0.23	4.6±0.33
22	3.9±0.90	3.9±0.73	2.1±0.50	2.7±0.90	2.1±0.50	1.9±0.80	5.1±0.20	5.2±0.20
35	2.7±1.50	2.6±0.60	2.3±0.70	2.4±1.00	2.2±1.50	1.9±2.10	4.7±0.90	2.3±0.42

Values represent mean K_d (nM) of [^{3}H] 8-OH-DPAT for 5-HT$_{1A}$ and [^{3}H] Ketanserin for 5-HT$_{2A}$ receptors in different regions of the brain after SFV infection ± s.e.m., n=4. Comparisons of saline versus SFV-infected mice were made by 2-way ANOVA. Individual comparisons were made at each age using Duncan's *post hoc* test. $P > 0.05$. PID=Post inoculation day.

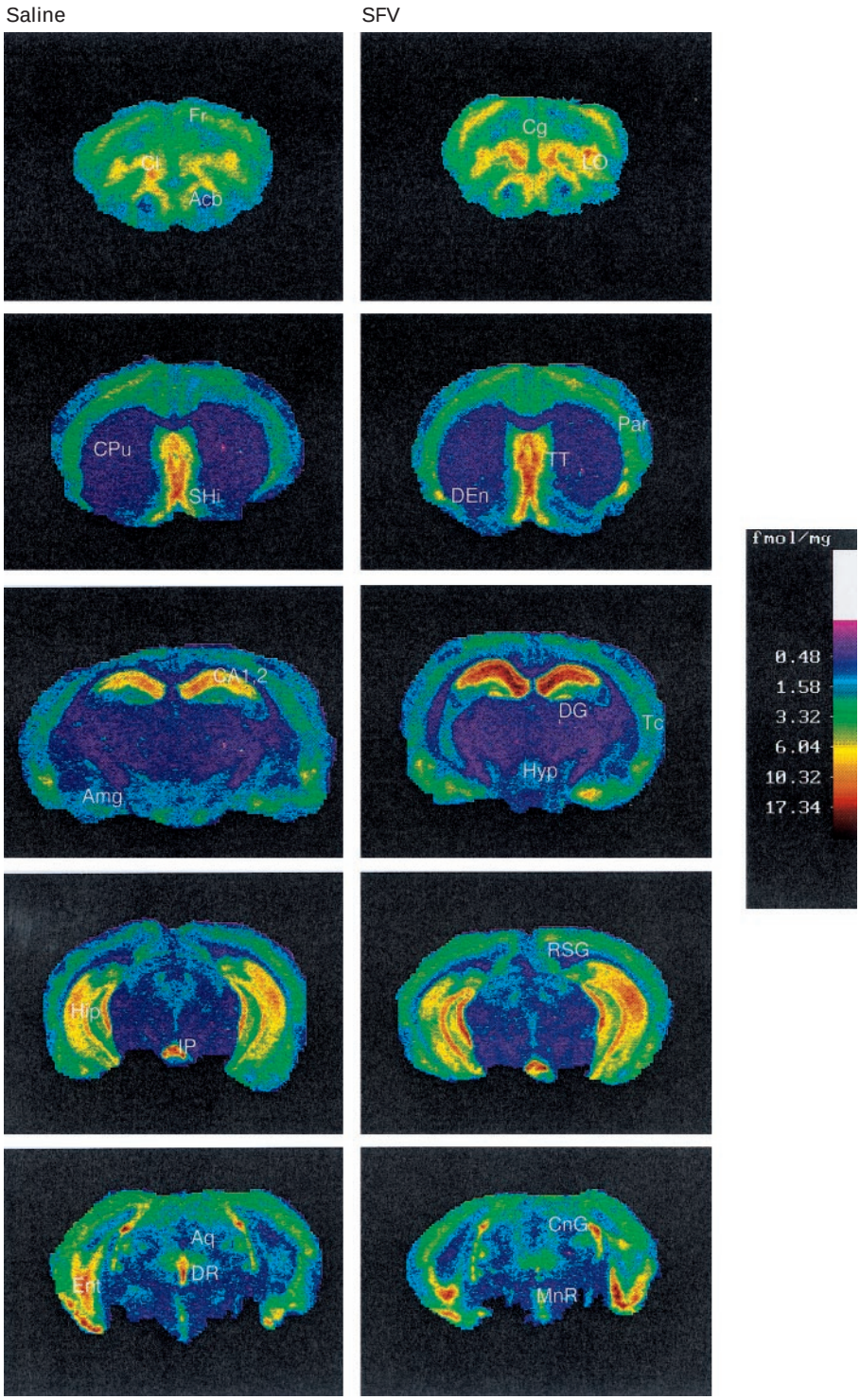

Figure 3 Computer enhanced colour autoradiograms of rostro-caudal coronal sections cut at the level of the forebrain and midbrain, showing 5-HT$_{1A}$ receptor binding with [^{3}H] 8-OH-DPAT in saline and SFV-infected tissue on post infection day 14. Quantitative analysis of SFV-infected sections (right column) show increase in 5-HT$_{1A}$ receptor binding compared to saline-treated sections (left column). Nonspecific images on the autoradiograms were at background levels. Areas identified are Aq, Aqueduct, Acb, nucleus accumbens, Amg, amygdaloid nuclei, CA1,2, two fields of hippocampus, Cg, cingulate cortex, Cl, claustrum, CnG, central gray, CPu, caudate putamen, DEn, Endopiriform nucleus, DG, dentate gyrus, DR, dorsal raphe, Ent, entorhinal cortex, Fr, frontal cortex, Hip, hippocampus, Hyp, hypothalamus, IP, interpeduncular nucleus, LO, lateral orbital cortex, MnR, medial raphe nucleus, Par, parietal cortex, RSG, retrosplenial granular cortex, SHi, Septohippocampal nucleus, Tc, temporal cortex, TT, tenia tecta.

Table 2 Quantitative autoradiography of 5-HT$_{1A}$ receptors in adult mouse brain sections labelled with [^{3}H] 8-OH-DPAT.

Region	*PID 6*		*PID 14*		*PID 22*	
	Saline	SFV	Saline	SFV	Saline	SFV
Olfactory system						
Ant. olf. n. *lateral*	12.0±0.5	13.0±0.8	13.2±0.3	15.3±0.3	10.0±0.3	9.5±0.5
Ant. olf. n. *ventral*	12.5±0.3	15.0±1.0	12.0±1.6	12.0±2.0	10.4±0.3	11.5±0.8
Basal ganglia						
N. accumbens	6.5±1.0	12.0±1.4*	6.4±2.1	14.0±3.0*	7.0±0.4	9.0±0.3
Septal region						
Tenia tecta	11.4±1.0	22.2±3.3*	8.4±1.5	16.4±1.3*	8.1±2.0	14.2±1.0*
Septohippocampal n.	12.3±2.0	27.0±2.0*	9.5±2.0	18.0±4.2*	10.4±2.4	11.3±1.5
Septum	17.0±3.5	29.0±3.0*	11.0±3.0	26.0±3.0*	10.4±1.0	16.0±3.0
Amygdala						
Med. amygdala n.	6.5±0.9	13.0±1.0*	5.2±0.2	12.0±0.6*	3.6±0.6	4.6±0.5
Baso. amygdala n.	5.3±1.0	14.0±1.0*	5.1±1.0	12.0±1.0*	5.3±1.0	8.4±0.2
Hippocampus						
Dentate gyrus	9.6±2.5	12.3±4.0	8.2±3.0	15.3±1.0	8.0±2.0	10.1±2.5
CA1 field	16.7±4.0	26.0±5.0*	14.2±4.0	28.0±6.0*	9.9±1.0	17.0±2.5*
CA2 field	13.0±3.0	22.0±5.0*	13.5±5.0	24.0±5.0*	7.6±1.0	16.0±2.0*
Whole hippocampus	10.1±4.0	19.0±4.0*	9.4±4.0	17.0±4.0*	6.8±2.0	14.0±2.0*
Hypothalamus						
Hypothalamus, whole	8.8±2.0	11.3±4.5	7.0±2.0	10.4±3.0	6.8±1.0	9.6±2.0
Ant. vent. preoptic n.	5.6±3.0	13.0±5.0*	4.8±1.0	13.0±2.0*	3.3±0.6	5.8±3.0
Cortical area						
Frontal cortex	11.0±0.3	24.0±2.0*	9.1±1.0	15.0±3.0*	9.5±1.0	18.0±2.0*
Lateral orbital cortex	12.0±2.5	22.0±2.0*	10.2±2.0	21.0±3.0*	8.8±2.0	19.0±2.0*
Parietal cortex	10.8±1.0	12.4±5.0	4.6±1.0	4.2±1.0	4.3±1.5	4.2±2.0
Piriform cortex	13.0±1.5	15.0±4.5	14.4±7.0	16.6±5.0	12.7±2.0	12.4±1.0
Claustrum	20.2±1.0	34.0±4.0*	15.1±2.0	32.0±5.0*	10.2±2.0	17.2±2.0
Cingulate cortex	9.6±1.0	12.3±2.0	6.1±3.0	13.6±6.0	9.5±1.0	11.6±5.0
Retrosplenial cortex	4.7±1.0	5.6±0.2	3.8±1.0	5.7±1.0	2.4±1.0	2.8±1.0
Oculomotor cortex	11.0±0.4	12.0±0.5	10.7±6.0	9.9±3.0	8.4±1.0	9.2±0.4
Tempral cortex	10.2±2.0	15.0±4.0	9.2±1.0	9.8±2.0	9.1±1.0	8.6±2.0
Entorhinal cortex	15.5±1.0	25.0±2.4*	10.6±6.0	21.0±4.0*	10.5±1.0	20.0±3.0*
Midbrain						
Interpeduncular n.	14.2±2.0	24.0±3.0*	13.0±0.4	24.0±3.0*	8.9±1.0	11.0±2.0
Central gray	3.5±1.0	4.7±1.0	4.4±2.0	6.9±0.6	4.7±1.0	5.8±1.0
Dorsal raphe n.	10.4±2.0	7.8±3.0	10.4±2.0	10.1±2.0	8.0±0.8	8.0±0.5
Median raphe n.	3.6±1.0	3.8±1.0	3.3±0.3	6.3±2.0	2.4±0.7	4.0±2.0

Quantitative autoradiography of 5-HT$_{1A}$ receptor binding in adult mouse brain after SFV-infection showing mean specific binding (n=3–4) in femtomoles per millgram of tissue±s.e.m., with regional determination made from both sides of sections, 400 μm apart. PID=post inoculation day. Labelling with [^{3}H] 8-OH-DPAT was carried out on adjacent sections and in a completely paired protocol. *Denotes significant difference from values found in saline-treated mice. Comparisons were made at each age by 1-way ANOVA followed by Duncan's *post hoc* test, $P<0.05$. Ant.=anterior, Baso=basolateral, Med=medial, n.=nucleus, Olf=olfactory, vent=ventral.

difference in density of binding between saline-treated and SFV-infected brains. The highest level of [^{3}H] Ketanserin binding was found in the frontoparietal cortex, claustrum and olfactory tubercles. Intermediate levels were detected in endopiriform nucleus, cingulate and temporal cortex, anterior olfactory nucleus, Island of Calleja, nucleus accumbens, caudate putamen and dorsal raphe nucleus. Lower levels were detected in septohippocampal nucleus, central gray, median raphe nucleus, ventral tegmental area, hippocampus, dentate gyrus and thalamus.

Effect of SFV infection on plasma corticosterone levels

Table 4 shows the plasma corticosterone levels in mice on various days after SFV infection. The plasma corticosterone levels in the saline-treated mice were between 100–112 μg/ml on days 2 to 22. In the SFV-infected mice the plasma corticosterone levels on days 2 were comparable to the saline-treated group. However, on days 6 and 22 after infection, the corticosterone levels were significantly lower (by 20%, $P<0.05$) compared to the saline-treated group.

Discussion

The autoradiographic mapping and parameters from homogenate binding for 5-HT$_{1A}$ and 5-HT$_{2A}$ are in good agreement with previously reported studies (Fitzgerald *et al*, 1993; Khawaja, 1995; Nebeshima *et al*, 1992; Pazos *et al*, 1985; Saavedra and Himeno, 1991). The results show clear upregulation of 5-HT$_{1A}$ receptors after SFV infection

which is not evident in 48 h but is marked 6 days after infection. Both the autoradiographic mapping and homogenate binding show this is reversible with normal levels returning by day 35. Although homogenate binding only showed significant upregulation in cortex the greater resolution afforded by autoradiography showed several fore and mid-brain structures where SFV infection caused upregulation. Whether this regional selectivity is dependent on the virus possessing a tropism for a particular neuronal type or area cannot be determined. The avirulent strain of SFV is found in small perivascular foci scattered around the brain (Fazakerley *et al*, 1993). However, a thorough neuroanatomical study has not been carried out to determine whether these foci are scattered only in particular areas or whether they are totally random occurring in all structures. SFV is detectable in the brain up

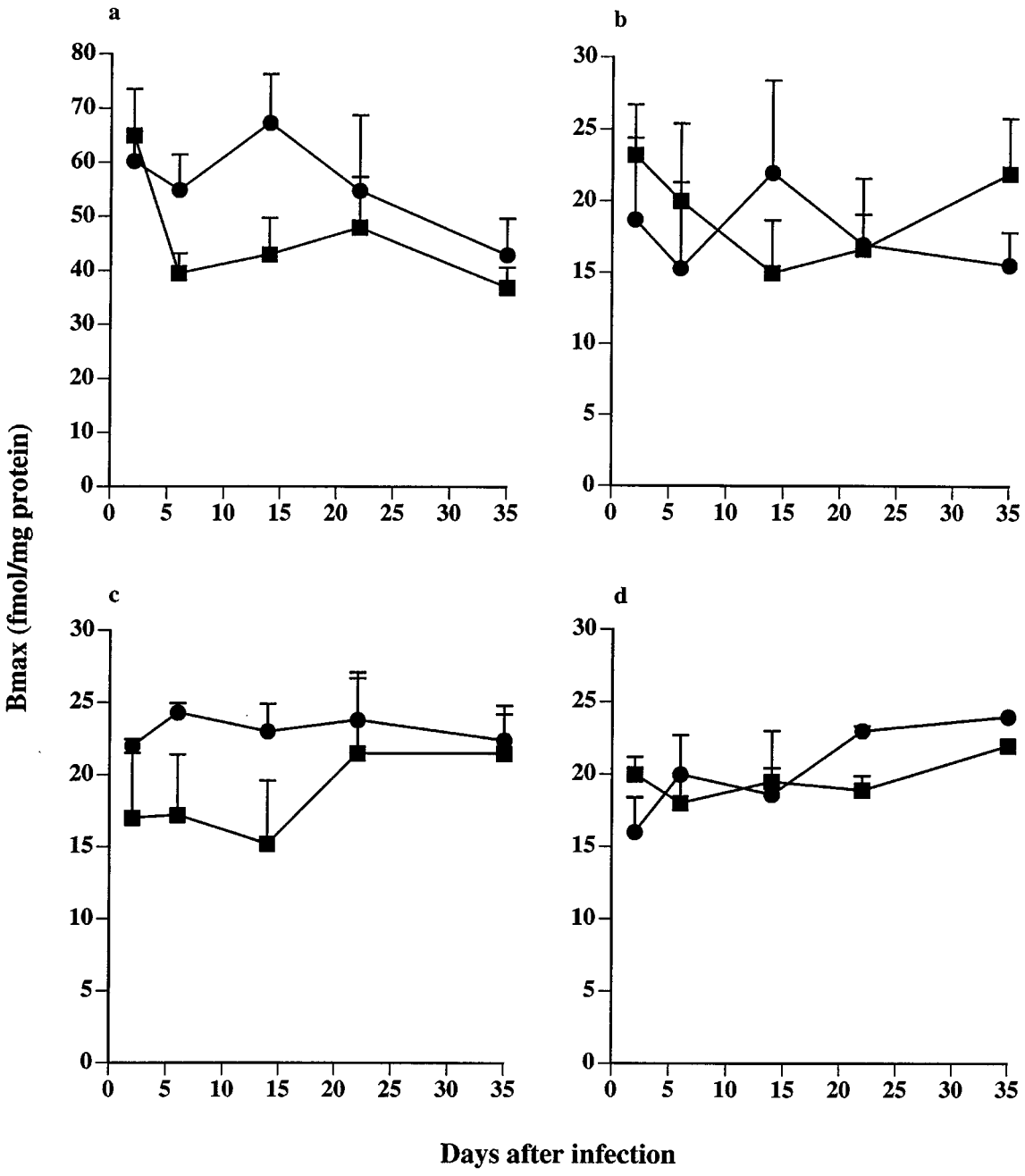

Figure 4 Time course of the effect of SFV on the number of 5-HT$_{2A}$ receptors labelled with [^{3}H] Ketanserin. Values represent Bmax (fmol/mg protein). (**a**) cortex, (**b**) midbrain, (**c**) hypothalamus, and (**d**) pons/medulla on various days after infection. ● SFV, ■ Saline. Comparisons were made by 2-way ANOVA. Specific comparisons of SFV and saline treatment were made at each age using Duncan's *post hoc* test. *n*=4. Error bars show s.e.m.

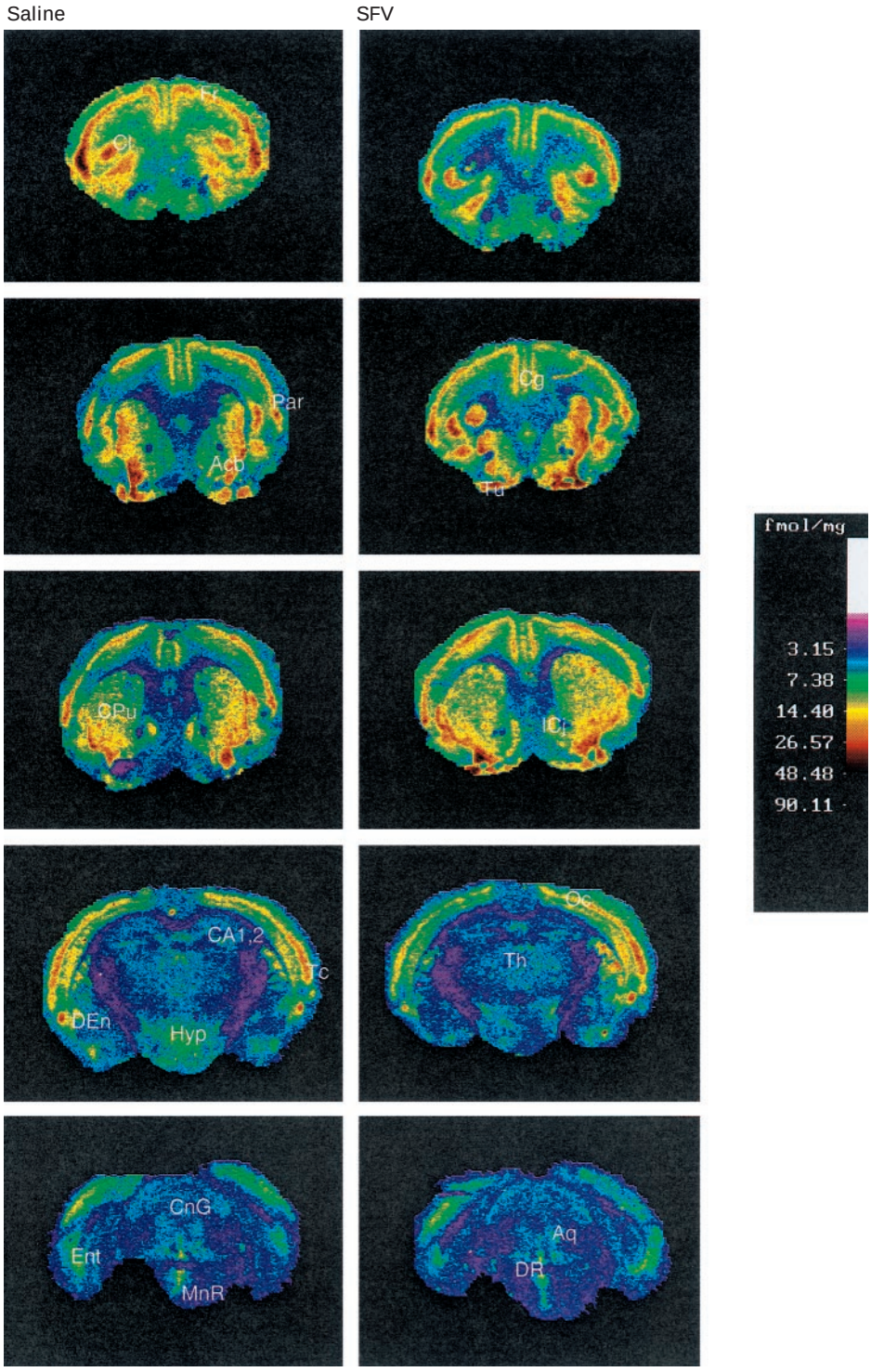

Figure 5 Computer enhanced colour autoradiograms of rostro-caudal coronal sections cut at the level of the forebrain and midbrain, showing 5-HT$_{2A}$ receptor binding with [^{3}H] Ketanserin in saline and SFV-infected tissue on post infection day 14. Quantitative analysis of SFV-infected sections (right column) show equivalent numbers of 5-HT$_{2A}$ receptors compared to saline-treated sections (left column). Nonspecific images on the autoradiograms were at background levels. Areas identified are Aq Aqueduct, Acb, nucleus accumbens, CA1,2, two fields of hippocampus, Cg, cingulate cortex, Cl, claustrum, CnG, central gray, CPu, caudate putamen, DEn, Endopiriform nucleus, DR, dorsal raphe, Ent, entorhinal cortex, Fr, frontal cortex, Hyp, hypothalamus, ICj, Island of Calleja, MnR, medial raphe nucleus, Oc, oculomotor cortex, Par, parietal cortex, Tc, temporal cortex, Th, Thalamus, Tu, olfactory tubercle.

Table 3 Quantitative autoradiography of 5-HT$_{2A}$ receptors in adult mouse brain sections labelled with [^{3}H] Ketanserin.

Region	PID 6		PID 14		PID 22	
	Saline	SFV	Saline	SFV	Saline	SFV
Olfactory system						
Ant. olfactory nucleus *lateral*	10.4±0.6	9.8±0.5	11.0±0.7	11.7±0.8	8.7±0.4	9.4±0.6
Ant. olfactory nucleus *ventral*	13.4±1.0	11.4±1.4	13.0±1.2	10.0±1.3	9.4±2.0	11.3±0.9
Olfactory tubercle	14.4±0.7	14.4±0.9	12.5±2.0	14.0±1.3	12.6±1.3	12.0±0.8
Island of Calleja	8.5±0.4	9.0±1.7	10.4±0.3	9.5±2.0	7.7±0.6	6.9±0.5
Basal ganglia						
Nucleus accumbens	13.4±2.2	11.5±1.0	14.7±2.0	13.6±1.0	13.0±0.7	10.0±9.0
Caudate putamen, whole	12.3±3.0	13.0±1.6	15.0±1.2	12.6±1.0	10.5±0.8	8.4±0.3
Septal region						
Septohippocampal nucleus	5.6±0.4	7.4±0.8	6.0±0.5	7.4±1.0	4.6±0.5	5.5±1.0
Hippocampus						
Dentate gyrus	6.0±0.4	7.2±0.4	6.0±0.5	7.4±1.0	5.7±0.4	4.3±0.8
Hypothalamus						
Medial mammilary nucleus	8.8±2.4	6.4±1.2	7.9±0.8	6.5±1.4	5.2±0.6	5.5±0.4
Ventral tegmental area	6.0±2.4	5.3±1.0	6.4±0.9	7.1±2.4	4.7±0.2	6.7±0.9
Thalamus						
Paraventricular nucleus	5.0±1.3	4.3±0.8	5.5±0.9	7.1±2.4	4.6±2.0	5.5±0.5
Cortical area						
Frontal cortex	22.6±1.8	25.0±2.6	26.8±1.5	25.0±2.2	20.8±1.6	21.0±1.7
Parietal cortex	20.5±1.6	22.4±2.9	24.0±1.4	22.0±4.2	19.0±1.4	20.0±2.4
Endopiriform nucleus	12.8±2.6	13.0±3.3	13.6±2.0	15.0±4.2	10.5±3.8	11.3±2.5
Claustrum	15.4±1.5	13.0±3.4	18.0±2.0	12.6±1.2	10.5±3.0	11.7±2.0
Cingulate cortex	11.0±3.0	12.5±1.6	14.0±0.9	12.5±2.0	10.0±2.2	8.9±1.4
Oculomotor cortex	7.9±0.8	8.8±1.2	8.0±0.3	10.0±2.0	5.8±2.0	6.6±1.4
Tempral cortex	12.6±1.3	11.9±1.0	11.7±1.0	14.2±1.0	9.4±1.6	9.0±2.5
Midbrain						
Central gray	4.8±0.3	3.3±0.4	5.0±0.4	4.3±1.0	5.0±0.9	4.6±0.8
Dorsal raphe nucleus	12.3±2.2	9.7±1.4	11.0±0.3	8.3±2.0	7.8±0.5	6.2±0.4
Median raphe nucleus	6.0±2.0	5.3±0.7	4.7±0.6	4.0±0.2	3.3±0.4	5.0±0.8

Quantitative autoradiography of 5-HT$_{2A}$ receptor binding in adult mouse brain after SFV-infection showing mean specific binding (n=3–4) in fmol/mg tissue±s.e.m., with regional determinations from both sides of sections, 400 μm apart. PID=post inoculation day. Labelling with [^{3}H] Ketanserin was carried out on adjacent sections and in a paired protocol. Comparisons were made at each age by 1-way ANOVA followed by Duncan's *post hoc* test, $P<0.05$. Ant=anterior.

Table 4 Effect of SFV on plasma corticosterone (μg/ml) levels in adult mice

Treatment	PID 2	PID 6	PID 22
SFV	97.0±6.3	78.0±6.8*	86.0±4.0*
Saline	104.0±4.9	107.0±7.4	112.0±7.7

Mean plasma corticosterone levels (mg/ml)±s.e.m. (n=4) in adult mice after SFV-infection. PID=post inoculation day. *Denotes significant difference ($P<0.05$) from values in saline-treated mice. Comparisons were made by 2-way ANOVA and specific comparisons of SFV and saline treatment were made at each age using Duncan's *post hoc* test.

to 10 days after infection and replicates predominantly in the neurons without altering cell morphology (Oaten *et al*, 1976; Pathak *et al*, 1983). This suggests that any changes occurring in K_d or B_{max} are not secondary to cell death. The changes induced by SFV infection are manifested not only at the time of virus replication but persist in the absence of virus for more than 10 days after the virus is not detectable in the brain.

The molecular mechanisms of upregulation of 5-HT$_{1A}$ receptor number in SFV infection remains to be elucidated although the lack of effect on K_d suggests that conformational changes do not occur. The delay in the effect of SFV infection in upregulating the 5-HT$_{1A}$ receptor might suggest an action at the mRNA level and the possibility of disruption of hormonal regulation of gene expression. It has been shown that corticosterone exerts direct control over 5-HT$_{1A}$ gene expression within the hippocampus (Chaouloff, 1995) and others have reported that abrogation of corticosterone by adrenalectomy increases binding of [^{3}H] 8-OH-DPAT to 5-HT$_{1A}$ receptors in CA1, CA2 and CA3 of the hippocampus (Mendelson and McEwen, 1992; Tejani-Butt and Labow, 1994). In our study we showed a small but significant decrease in corticosterone levels in SFV-treated animals and it is possible that this contributes to 5-HT$_{1A}$ upregulation at levels of gene expression. Furthermore, upregulation of 5-HT$_{1A}$ receptors in experimental models of depression show a 8-OH-DPAT induced hypothermic response in mice and that administration of

corticosterone produces attenuation of this hypothermia via 5-HT$_{1A}$ receptors (Young *et al*, 1994). Other viruses have been reported to alter plasma corticosterone and ACTH levels in mice and enhanced adrenocortical activity has been shown for Newcastle and influenza virus, associated with increased levels of noradrenaline metabolites (Dunn, 1989; Dunn and Vickers, 1994). These responses may reflect stress-induced effects of these viruses but the inhibition of corticosterone after SFV would suggest that stress *per se* is not a factor in the action of this virus on 5-HT$_{1A}$ receptors. Further it is also unlikely that the effects of SFV infection on 5-HT$_{1A}$ receptors reflect changes in 5-HT levels since we have previously shown a lack of effect of this virus on steady state 5-HT content in the brain (Mehta *et al*, 1993). In relation to this, it is possible that the upregulation of 5-HT$_{1A}$ receptors may be selective for the postsynaptic 5-HT$_{1A}$ sites since it would be anticipated that effects on the somatodendritic 5-HT$_{1A}$ receptors would alter 5-HT release (Descarries *et al*, 1990; Lee *et al*, 1979).

Another possible mechanism by which upregulation of 5-HT$_{1A}$ receptors may take place is indirectly through the immune system and a number of recent studies have demonstrated links between neurotransmitters and the immune system. During SFV infection, enhanced expression of interleukins, IL-1, IL2, IL3, IL4, IL6 and IL10 have been detected in the brain and in particular, a higher density of IL-1α is detected between days 14 and 35 after infection, predominantly around inflammatory areas including the meninges (Morris *et al*, 1997). Autoradiographic studies show that IL-1α receptors are localized in specific areas of the brain such as dentate gyrus, fronto-parietal cortex, choroid plexus, meninges and the anterior pituitary (Ban, 1994) and as these regions do not exactly correspond with those where 5-HT$_{1A}$ receptors show upregulation the possibility of interaction with other cytokines must also be considered a possibility. For example, in mice, IL-1β has been shown to enhance 5-HT turnover in the hippocampus and the prefrontal cortex (Zalcman *et al*, 1994) and in rats, intrahippocampal administration of IL-1β has shown to increase extracellular 5-HT levels in the hippocampus (Linthorst *et al*, 1994). The effects of SFV on hippocampal 5-HT$_{1A}$ receptors are particularly striking and the changes here may be secondary to activation of IL-1β. This possibility should be viewed with caution since IL-1β has also been shown to inhibit 5-HT$_{2A}$ receptor-mediated Ca^{2+} mobilization (Kugaya *et al*, 1995) and yet 5-HT$_{2A}$ receptors were clearly not influenced by SFV-infection in our study. Nevertheless, it is possible that the upregulation of 5-HT$_{1A}$ during SFV infection may be induced by the interaction between 5-HT and cytokines or other components of the immune system. In this regard 5-HT has been reported to modulate T cell and NK cell proliferation and it has been shown that 5-HT upregulated mitogen-stimulated B lymphocyte proliferation through 5-HT$_{1A}$ receptors (Iken *et al*, 1995). A further study using severely compromised immunodeficient (SCID) mice would show whether the immune system plays any part in the upregulation of 5-HT$_{1A}$ receptors during SFV infection since IL-1β is detected in the CNS of SCID mice infected with Sindbis virus, a virus closely related to SFV (Wesselingh *et al*, 1994).

The autoradiographic mapping showing regional upregulation of 5-HT$_{1A}$ receptors also suggests that during SFV infection two different neuronal pathways may be affected, one which include the septo-hippocampo-peduncular pathway (Waeber *et al*, 1994) and the other which include the frontocortical-claustrum-septo-amygdala pathway (Van Bockstaele *et al*, 1993; Vertes, 1991). These pathways are known to be involved in memory, learning, and emotions and in cognitive functions and motor activity (Lee *et al*, 1992; Ogren, 1995; Ogren *et al*, 1985; Warbritton *et al*, 1978).

The autoradiographic mapping of 5-HT$_{2A}$ shows a distinct distribution from 5-HT$_{1A}$ receptors but in the few regions where 5-HT$_{2A}$ and 5-HT$_{1A}$ receptors are co-localised such as the claustrum, nucleus accumbens, frontal and cingulate cortex there is no indication of any effect of SFV on 5-HT$_{2A}$ receptor number. It is therefore clear that during SFV infection 5-HT$_{1A}$ sites are selectively targeted.

In conclusion, we have shown that SFV infection in mice induces a regionally selective upregulation of 5-HT$_{1A}$ but not 5-HT$_{2A}$ receptors without changes in receptor affinity. This upregulation represents virtually a doubling of site number notably in cortical regions, nucleus accumbens, hippocampus and septal regions which persists for 2–3 weeks after infection.

Materials and methods

Mice and virus infection

Inbred 3–4 week old BALB/c adult male mice (Bantin and Kingman Ltd, 19–24 g) were used. Animals were housed in air-conditioned unit maintained at 20°C+1°C and 50–60% humidity with light control on a 12 h cycle (lights off 19.00 h–07.00 h) and allowed free access to food and water. The avirulent strain A7(74) of SFV was suspended in 0.75% bovine albumin phosphate saline (BAPS) and stored at −70°C until used. The mice in the infected group were inoculated intraperitoneally (i.p.) with a dose of 10^4 suckling mouse intracerebral LD_{50}, contained in 0.1 ml of BAPS. The mice in the control group received 0.1 ml BAPS only by the i.p. route.

Homogenate binding

5-HT$_{1A}$ and 5-HT$_{2A}$ receptors were labelled with [^{3}H] 8-OH-DPAT and [^{3}H] Ketanserin respectively.

These ligands have been used extensively and are recognised to have appreciable selectivity for these 5-HT subtypes (Hoyer *et al*, 1994).

Whole brains were removed from each group on post inoculation day (PID) 2, 6, 14, 22 and 35. Each individual saturation study represents pooled tissue from 10 mice. The mice were killed by cervical dislocation and the whole brain removed immediately and placed in a Petri dish on ice. Four regions of the brain (cortex, midbrain, pons/medulla and hypothalamus) were dissected out and placed in a pre-weighed beaker containing ice cold 50 mM Tris-HCl, pH 6.8. The tissues were weighed and homogenised in fresh ice cold 50 mM Tris-HCl pH 6.8 buffer using a polytron, followed by centrifugation at 36 500 × g for 15 min. The resulting pellets were resuspended in 50 mM Tris-HCl, pH 7.7 and homogenised prior to preincubation in the same buffer at 37°C for 30 min to remove endogenous 5-HT. The homogenates were then centrifuged at 36 500 × g for a further 15 min and the pellets resuspended at a concentration of 10 mg/ml in the final homogenisation buffer (50 mM Tris-HCl, pH 7.7) containing $CaCl_2$ (4 mM, ascorbic acid (0.1%) and pargyline (1 μM).

The binding of [^{3}H] 8-hydroxy-2-(di-n-propylamino)-tetralin ([^{3}H] 8-OH-DPAT) (Amersham, UK) and [^{3}H] Ketanserin (Du Pont, NEN, UK) in duplicate, was determined using 10 ligand concentrations for [^{3}H] 8-OH-DPAT (0.25 – 12 nM) and for [^{3}H] Ketanserin (1 – 12 nM). The binding at each concentration was measured in the presence and absence of 10 μM 5-HT (Sigma, UK) (for 5-HT$_{1A}$) and 10 μM ketanserin (RBI, UK) (for 5-HT$_{2A}$) in order to determine the non-specific and total binding respectively. Binding assays were carried in 50 mM Tris-HCl buffer containing $CaCl_2$ (4 mM), ascorbic acid (0.1%) and pargyline (1 μM) at 37°C for 15 min for [^{3}H] 8-OH-DPAT and 30 min for [^{3}H] Ketanserin. Assays were terminated by filtration through Whatman GF/B filters, using a Brandel M-24 cell harvester, washing three times with 4 ml of ice-cold Tris-HCl buffer and radioactivity determined by liquid scintillation spectrometry.

Autoradiography

Mice were killed on PID 6, 14 and 22 by decapitation and brains removed, frozen at −20°C in isopentane and stored at −70°C for a maximum of 1 month. For autoradiographic mapping, 20 μm frozen coronal sections were cut (400 μm apart) in a cryostat at −20°C and thawmounted onto gelatin-coated slides and stored for one week at −20°C. Frozen sections were brought to room temperature 30 min prior to ligand binding assay and thereafter preincubated in 170 mM Tris-HCl buffer (pH 7.4) containing $CaCl_2$ (4 mM), ascorbic acid (0.1%) and pargyline (1 μM) for 30 min at room temperature. Binding was carried out using 1 ml of the same buffer containing 4 nM [^{3}H] 8-OH-DPAT or 4 nM [^{3}H] Ketanserin, incubated for 30 min or 60 min respectively. Non-specific binding was determined on adjacent sections by the addition of 3 μM 5-HT (for 5-HT$_{1A}$) or 3 μM Ketanserin (for 5-HT$_{2A}$). Sections were then washed for 5 min in ice-cold buffer three times followed by a brief immersion in ice-cold distilled water. The sections were dried under a stream of cold air and desiccated at room temperature for 3 days. Autoradiograms were generated by apposing the labelled sections to [^{3}H] Hyperfilm (Amersham, UK). Films were developed in 50% Kodak D-19 (3 min) after 11 days ([^{3}H] 8-OH-DPAT) and 3 weeks ([^{3}H] Ketanserin) exposure at room temperature.

Plasma corticosterone studies

Adult BALB/c mice from saline-treated and SFV-infected groups were killed by decapitation, between 09.00 h and 10.00 h on post inoculation day 2, 6 and 22. Blood was drawn from the cardiac tissue and heparinised. Plasma was separated after centrifugation and stored at −20°C. Analysis of corticosterone was performed by the method of Sudo (1990). Briefly, 0.5 ml of plasma was transferred to a 50 ml stoppered glass tube and a known amount of tetrahydrocorticosterone (5B-pregnane-3,11B,21-triol-20-one) was added as an internal standard. The mixture was extracted with 15 ml of dichloromethane which was then washed with 2 ml of 0.1 M sodium hydroxide and then with 2.5 ml of water. At each extraction stage, the supernatant was tested for tetrahydrocorticosterone loss and taken into consideration when calculating the concentration of the internal standard. A 10 ml portion of the washed extract was evaporated to dryness at 45°C. The residue was dissolved in 0.5 ml acetonitrile and analysed by HPLC (Perkin Elmer integral series 4000) with UV detection. Steroid separation was carried out on 220 × 46 mm RP-C18 Spheri (Kontron, Switzerland) column packed with 5-μm particle size, at 30°C and a flow rate of 1.2 ml/min. The mobile phase was composed of acetonitrile HPLC grade and water (70 : 30% v/v). Before using the mobile phase, water was purified through a HA filter (Millipore) with 0.45 μm diameter pores. Eluted steroids were detected by UV absorbance at 254 nm. The concentration of corticosterone was calculated from the peak heights and area of both the steroid and the internal standard.

Quantitative analysis and statistical procedures

Data from saturation experiments were computed by Scatchard analysis. Measures of B_{max} were calculated per mg wet weight and mg protein. Protein concentrations were determined from aliquots of membrane homogenates by the method of Lowry *et al* (1951) using bovine serum albumin as standard. Comparisons of K_d and B_{max} were carried out using 1-way ANOVA followed by post-hoc analysis using Duncan's multiple range test. Quan-

titative analysis of receptor binding autoradiograms was carried out by video-based computerised densitometry using an MCID image analyser (Imaging Research, Canada). fmol/mg tissue equivalents for receptor binding were derived from [^{3}H]-microscale based calibrations (Amersham, UK) laid down with each film after subtraction of non-specific binding images which were at the level of background. For each region, quantified measures were taken from both right and left sides of brain. Comparisons of quantitative measures of autoradiographic binding for each ligand in saline-treated and SFV infected groups were carried out using one-way ANOVA followed by *post-hoc* analysis using Duncan's new multiple range test.

Acknowledgements

We are grateful to St Thomas' Charitable Trust and The Linbury Trust for their financial support.

References

Bakheit AMO, Behan PO, Dinan TG, Gray CE, O'Keane V (1992). Possible upregulation of hypothalamic 5-HT receptors in patients with post viral fatigue syndrome. *Br Med J* **304:** 1010–1012.

Ban EMH (1994). Interleukin-1 receptors in the brain: Characterization by quantitative *in situ* autoradiography. *Immunomethods* **5:** 31–40.

Baxter G, Kennett G, Blaney F, Blackburn T (1995). 5-HT$_2$ receptor subtypes: a family re-united. *Trends Pharmacol Sci* **16:** 105–110.

Ceccaldi PE, Fillion MP, Ermine A, Tsiang H, Fillion G (1993). Rabies virus selectively alters 5-HT1 receptor subtypes in rat brain. *Eur J Pharmacol* **245:** 129–138.

Chaouloff F (1995). Regulation of 5-HT receptors by corticosteroids. Where do we stand? *Fundam Clin Pharmacol* **9:** 219–233.

Descarries L, Audet MA, Doucet G, Garcia S, Oleskevich S, Seguela P, Soghomonian JJ, Watkins KC (1990). Morphology of central serotonin neurons: brief review of quantified aspects of their distribution and ultrastructural relationships. *Ann NY Acad Sci* **600:** 81–92.

Dunn AJ, Powell ML, Meitin C, Small PA (1989). Virus infection as a stressor: influenza virus elevates plasma concentration of corticosterone and brain concentrations of MHPG and tryptophan. *Physiol Behav* **45:** 591–594.

Dunn AJ, Vickers SL (1994). Neurochemical and neuroendocrine responses to Newcastle disease virus administration in mice. *Brain Res* **645:** 103–112.

Fazakerley J, Amor S, Webb HE (1983). Reconstitution of Semliki Forest virus infected mice, induces immune mediated pathological changes in the CNS. *Clin Expt Immunol* **52:** 115–120.

Fazakerley J, Pathak S, Scallan M, Amor S, Dyson H (1993). Replication of the A7(74) strain of Semliki Forest virus is restricted to neurons. *Virology* **195:** 627–637.

Fitzgerald LW, Ratty AK, Teitler M, Gross KW, Glick SD (1983). Specificity of behavioural and neurochemical dysfunction in the chakragati mouse: a novel genetic model of a movement disorder. *Brain Res* **608:** 247–258.

Gow JW, Behan PO, Clements GB, Woodall C, Millar J, More IA (1991). Enteroviral sequences detected by polymerase chain reaction in muscle biopsis of patients with postviral fatigue syndrome. *Br Med J* **302:** 692–696.

Grahame-Smith DG (1992). An overview of serotonin and psychiatry. In: *Serotonin 1A receptors in depression and anxiety*. Stahl SM, Gastpov M, Keppel-Hessellink JM *et al*, (eds) Raven Press, New York: pp 1–21.

Hoyer D, Clarke DE, Fozard JR, Hartig PR, Martin GR, Mylecharane EJ, Saxena AP, Humphrey PPA (1994). International Union of Pharmacology Classification of Receptors for 5-hydroxytryptamine (Serotonin). *Pharmacol Rev* **46:** 157–203.

Iken K, Chheng S, Fargin A, Goulet AC, Kouassi E (1995). Serotonin upregulates mitogen-stimulated B lymphocyte proliferation through 5-HT1A receptors. *Cell-Immunol* **163:** 1–9.

Illavia SJ, Webb HE (1988). The pathological effect on the central nervous system of mice following single and repeated infections of the demyelinating A7(74) strain of Semliki Forest virus. *Neuropath Appl Neurobiol* **14:** 207–220.

Illavia SJ, Webb HE, Pathak S (1982). Demyelination induced in mice by avirulent Semliki Forest virus. 1. Virology and effects on optic nerve. *Neuropath Appl Neurobiol* **8:** 35–42.

Khawaja X (1995). Quantitative autoradiographic characterisation of the binding of [3H] WAY-100635, a selective 5-HT1A receptor antagonist. *Brain Res* **673:** 217–225.

Kugaya A, Kagaya A, Uchitomi Y, Motohashi N, Yamawaki S (1995). Inhibition of serotonin-induced Ca2+ mobilization by interleukin-1 beta in rat C6BU-1 glioma cells. *Brain Res* **682:** 151–156.

Lee AJ, Fernando JCR, Curzon G (1979). Serotonergic involvement in behavioural response to amphetamine at high dosage. *Neuropharmacology* **8:** 153–158.

Lee EH, Lin WR, Chen HY, Shui WH, Liang KC (1992). Fluoxetine and 8-OH-DPAT in the lateral septum enhances and impairs retention of an inhibitory avoidance response in rats. *Physio Behav* **51:** 681–688.

Linthorst ACE, Flachskamm C, Holsboer F, Reul JMHM (1994). Local-administration of recombinant human interleukin-1 beta in the rat hippocampus increases serotonergic neurotransmission, hypothalamic-petuitary-adrenocortical axis activity, and body temperature. *Endocrinol* **135:** 520–532.

Lowry OH, Rosebrough NJ, Randall RJ (1951). Protein measurement with the Folin phenol reagent. *J Biol Chem* **93:** 265–275.

Mehta S, Parsons LM, Webb HE (1993). Effect of amitryptyline on neurotransmitter levels in adult mice following infection with the avirulent strain of Semliki Forest virus. *J Neurological Sci* **116:** 110–116.

Mendelson SD, McEwen BS (1992). Quantitative autoradiographic analysis of the time course and reversibility of corticosterone-induced decrease in binding at 5-HT$_{1A}$ receptors in rat forebrain. *Neuroendocrinology* **56:** 881–888.

Mohammed AK, Magnusson O, Maehlen J, Fonnum F, Norrby E, Schultzberg M, Kristensson K (1990). Behavioural deficits and serotonin depletion in adult rats after transient infant nasal viral infection. *Neuroscience* **35:** 355–363.

Morris MM, Dyson H, Baker D, Harbige LS, Fazakerly JK, Amor S (1997). Characterization of the cellular and cytokine response in the central nervous system following Semliki Forest virus infection. *J Neuroimmunol* **74:** 185–197.

Natelson BH, Ye N, Moul DE, Jenkins FJ, Oren DA, Tapp WN, Cheng Y (1994). High titres of anti-Epstein-Barr virus DNA polymerase are found in patients with severe fatiguing illness. *Br Med Virol* **42:** 42–46.

Nebeshima T, Hiramatsu M, Niwa K, Fuji K, Kameyama T (1992). Effect of naftidrofuryl oxalate on 5-HT$_2$ receptors in mouse brain: evaluation based on quantitative autoradiography and head-twitch response. *Eur J Pharmacol* **223:** 109–115.

Oaten SW, Webb HE, Bowen ETW (1976). Enhanced resistance of mice to infection with Langat (TP21) virus following pretreatment with Sindbis or Semliki Forest virus. *J Gen Virol* **33:** 381–388.

Ogren SO (1985). Evidence for a role of brain serotonergic neurotransmission in avoidance learning. *Acta Physiol Scand* **125:** 1–71.

Ogren SO, Johansson C, Magnusson O (1985). Forebrain serotonergic involvement in avoidance learning. *Neurosci Lett* **58:** 305–309.

Paivarinta MA, Marttila RJ, Rinne JO, Rinne UK (1992). Decrease in mesencephalic dopamine autoreceptors in experimental herpes simplex encephalitis. *J Neural Transm* **89:** 71–80.

Pathak S, Illavia SJ, Webb HE (1983). The identification and role of cells involved in CNS demyelination in mice after Semliki Forest virus infection: an ultrastructural study. *Prog Brain Res* **58:** 237–254.

Pazos A, Cortes R, Palacios JM (1985). Quantitative autoradiographic mapping of serotonin receptors in the rat brain. 11. Serotonin-2 receptors. *Brain Res* **346:** 231–249.

Saavedra JM, Himeno A (1991). Autoradiographic studies of 5-HT$_{2A}$ receptors. *Adv Exp Med Biol* **294:** 107–113.

Sudo A (1990). Analysis of corticosterone in rat urine by high performance liquid chromatography and fluorimetry using post-column reaction with sulphuric acid. *J Chromatography* **528:** 453–458.

Tejani-Butt SM, Labow DM (1994). Time course of the effects of adrenalectomy and corticosterone replacement on 5-HT1A receptors and 5-HT uptake sites in the hippocampus and dorsal raphe nucleus of the rat brain: an autoradiographic analysis. *Psychopharmacology-Berl* **113:** 481–486.

Van Bockstaele EJ, Biswas A, Pickel VM (1993). Topography of serotonin neurons in the dorsal raphe nucleus that send axon collaterals to the rat prefrontal cortex and nucleus accumbens. *Brain Res* **624:** 188–198.

Vertes RP (1991). A PHA-L analysis of ascending projections of the dorsal raphe nucleus in the rat. *J Comp Neurol* **313:** 643–668.

Waeber C, Sebben M, Nieoullon A, Bockaert J, Dumuis A (1994). Regional distribution and ontogeny of 5-HT4 binding sites in rodent brain. *Neuropharmacology* **33:** 527–541.

Warbritton JD, Stewart RM, Baldessarini RJ (1978). Decrease locomotor activity and attenuation of amphetamine hyperactivity with intraventricular infusion of serotonin in the rat. *Brain Res* **143:** 373–382.

Wesselingh SL, Levine B, Fox RJ, Choi S, Griffin DE (1994). Intracerebral cytokine mRNA expression during fatal and nonfatal alphavirus encephalitis suggests a predominant type 2 T cell response. *J Immunol* **152:** 1289–1297.

Whitaker-Azmitia P, Peroutka S (1990). The neuropharmacology of serotonin. *Ann Rev Clin Biochem* **31:** 462–467.

Young AH, Goodwin GM, Dick H, Fink G (1994). Effects of glucocorticoids on 5-HT$_{1A}$ presynaptic function in mouse. *Psychopharmacology-Berl* **114:** 360–364.

Zalcman S, Green-Johnson JM, Murray L, Nance DM, Dyck D, Anisman H, Greenberg AH (1994). Cytokine-specific central monoamine alterations induced by interleukin-1, 2 and 6. *Brain Res* **643:** 40–49.